Original Article

Preliminary study of apatinib combined with fluzoparib in the treatment of HRP ovarian cancer via the HR pathway

Lei Gao[1#], Sixing Wang[1#], Xintong Hu[1#], Lixia Wang[2], Yanfeng Xi[2], Peng Bu[2], Guohai Zhao[2], Lili Zhao[3], Yongming Yang[3], Hongwei Zhao[4]

[1]The Second Clinical Medicine, Shanxi Medical University, Taiyuan, China; [2]Department of Pathology, Shanxi Province Cancer Hospital/Shanxi Hospital Affiliated to Cancer Hospital, Chinese Academy of Medical Sciences/Cancer Hospital Affiliated to Shanxi Medical University, Taiyuan, China; [3]Laboratory Animal Center, Shanxi Province Cancer Hospital/Shanxi Hospital Affiliated to Cancer Hospital, Chinese Academy of Medical Sciences/Cancer Hospital Affiliated to Shanxi Medical University, Taiyuan, China; [4]Gynecological Oncology Department, Shanxi Province Cancer Hospital/Shanxi Hospital Affiliated to Cancer Hospital, Chinese Academy of Medical Sciences/Cancer Hospital Affiliated to Shanxi Medical University, Taiyuan, China

Contributions: (I) Conception and design: L Gao, S Wang, X Hu, H Zhao; (II) Administrative support: H Zhao; (III) Provision of study materials or patients: Y Xi, L Wang, Y Yang, H Zhao; (IV) Collection and assembly of data: L Gao, S Wang, P Bu, G Zhao; (V) Data analysis and interpretation: L Gao, S Wang, X Hu, L Zhao; (VI) Manuscript writing: All authors; (VII) Final approval of manuscript: All authors.

[#]These authors contributed equally to this work.

Correspondence to: Hongwei Zhao, PhD. Gynecological Oncology Department, Shanxi Province Cancer Hospital/Shanxi Hospital Affiliated to Cancer Hospital, Chinese Academy of Medical Sciences/Cancer Hospital Affiliated to Shanxi Medical University, Xinghualing District, Worker's New Street No. 3, Taiyuan 030013, China. Email: inmind20060829@126.com.

Background: Ovarian cancer is the gynecological malignancy with the highest mortality rate. Due to late detection and easy recurrence, the 5-year survival rate of advanced ovarian cancer patients is less than 30%. The current standard treatment for ovarian cancer includes platinum-based combination therapy. Most ovarian cancer patients achieve clinical remission; however, the short-term recurrence rate is still high. For patients with recurrent ovarian cancer, who are unwilling to receive chemotherapy or cannot tolerate chemotherapy after multiple lines of chemotherapy, "chemotherapy-free" treatment may be appropriate. This study aimed to investigate the preliminary mechanism of action of the antiangiogenic drug apatinib combined with poly ADP ribose polymerase (PARP) inhibitor fluzoparib as a "chemotherapy-free" regimen in the treatment of ovarian cancer patients with homologous recombination proficiency (HRP).

Methods: The HRP cell line SKOV3 was used for the experiments. The cells were treated with apatinib, fluzoparib, and apatinib combined with fluzoparib, respectively. The cell proliferation rate and migration rate were detected by 3-(4,5-dimethyl-2-thiazolyl)-2,5-diphenyl-2-H-tetrazolium bromide (MTT) and scratch assays. Western blot was used to detect the expression of phosphorylated mitogen-activated protein kinase kinase (*p-MEK*), recombination activating gene 51 (*RAD51*), and phosphorylated histone cluster 2 H2A family member X (*γH2AX*). Animal experiments were performed to evaluate the effects of the combined therapy on tumor growth and drug toxicity by constructing a cell-line transplanted tumor model. Western blot was used to detect the expression of *p-MEK*, *RAD51*, and *γH2AX*. Immunohistochemistry (IHC) was used to detect the expression of *γH2AX*, phosphorylated extracellular signal-regulated kinase (*p-ERK*), and breast cancer 1 *(BRCA1*).

Results: *In vitro*, apatinib combined with fluzoparib significantly inhibited the growth and migration of the SKOV3 cells. Western blot showed that apatinib combined with fluzoparib induced the down-regulation of *p-MEK* and homologous recombination (HR) pathway-related protein *RAD51* expression, and increased DNA damage-related protein *γH2AX* expression in the SKOV3 cells. The animal experiment results showed that apatinib combined with fluzoparib had a better antitumor effect than single-drug therapy without obvious *in vivo* toxicity. The western blot results showed that *γH2AX* protein expression was increased, and *p-MEK* protein expression was decreased in the apatinib combined with fluzoparib group. The IHC results showed that *γH2AX* protein expression was increased and *p-MEK* protein expression was decreased in the

apatinib combined with fluzoparib group.

Conclusions: The combination of apatinib and fluzoparib may cause changes in the HR pathway by down-regulating *MEK* signaling in ovarian cancer, leading to the down-regulation of *RAD51*. This eventually leads to the increased expression of DNA damage-related protein *γH2AX*, which plays a therapeutic role in ovarian cancer *in vitro* and *in vivo*.

Keywords: Ovarian cancer; apatinib; fluzoparib; homologous recombination pathway (HR pathway)

Submitted Mar 26, 2025. Accepted for publication Apr 22, 2025. Published online Apr 27, 2025.
doi: 10.21037/tcr-2025-666
View this article at: https://dx.doi.org/10.21037/tcr-2025-666

Introduction

Ovarian cancer is the most common malignant tumor among women, and a high number of new cases are reported every year (1). Approximately half of ovarian cancer cases have homologous recombination deficiency (HRD) while the other half have normal homologous recombination proficiency (HRP) (2,3).

Most patients with early-stage ovarian cancer achieve clinical remission after surgery and chemotherapy; however, the short-term recurrence rate remains very high, primarily due to the development of chemotherapy resistance. Moreover, conventional chemotherapy is not suitable for every patient. Patients who do not wish to undergo chemotherapy or who do not tolerate the toxicity of chemotherapy can opt for "chemotherapy-free", and current "chemotherapy-free" therapies are mostly focused on PARP inhibitors (4).

PARP inhibitors have shown promising antitumor activity in patients with impaired HR repair. Single-agent PARP inhibitors are particularly effective in ovarian cancer patients with *BRCA1* or *BRCA2* mutations, or those positive for HRD. However, the benefit for HRP ovarian cancer patients is very limited (5). Thus, research needs to be conducted to determine how HRP ovarian cancer patients can benefit from PARP inhibitors.

A previous study has shown that the PARP inhibitor olaparib combined with the antiangiogenic agent cediranib has an antitumor activity similar to that of platinum-based chemotherapy agents (6). The National Comprehensive Cancer Network Clinical Practice Guidelines in Oncology also note that PARP inhibitors can be used in combination with other non-chemotherapy drugs, such as antiangiogenic targeted therapy, to establish an effective individualized "chemotherapy-free" regimen (7,8).

Targeting the DNA damage response in tumors with defective DNA repair is a successful clinical strategy. The RAS/RAF/MEK/ERK signaling pathway is frequently dysregulated in human cancers. The MEK1/2 branch of the MAPK pathway primarily stimulates cell proliferation,

Highlight box

Key findings

- The combination of apatinib and fluzoparib may cause changes in the homologous recombination (HR) pathway by down-regulating mitogen-activated protein kinase kinase (*MEK*) signaling in ovarian cancer, leading to the down-regulation of *RAD51*. This eventually leads to the increased expression of DNA damage-related protein *γH2AX*, which plays a therapeutic role in ovarian cancer *in vitro* and *in vivo*.

What is known, and what is new?

- Some clinical studies have shown that olaparib in combination with cediranib exerts antitumor activity similar to that of platinum-based chemotherapy treatments; thus, combining antiangiogenic drugs with poly ADP ribose polymerase (PARP) inhibitors as an alternative to platinum-based chemotherapy represents an interesting treatment approach. PARP inhibitors have been shown to improve survival in ovarian cancer patients with breast cancer 1/2 (*BRCA1/2*) mutations or homologous recombination deficiency (HRD); however, the benefit in patients with homologous recombination proficiency (HRP) is very limited. Further research needs to be conducted to determine how HRP ovarian cancer patients can benefit from "chemotherapy-free" treatment.
- Thus, this study investigated the antitumor activity of fluzoparib, a PARP inhibitor, and apatinib, an antiangiogenic agent, and compared them with chemotherapeutic agents to analyze their intrinsic mechanism of action to expand the scope of action of PARP inhibitors and provide an emerging "chemotherapy-free" option for HRP ovarian cancer patients.

What is the implication, and what should change now?

- Further in-depth research needs to be conducted, and the expression of the downstream signalling of the mitogen-activated protein kinases (*MAPK*) pathway and the deep mechanism need to be further examined in corresponding experiments.

migration, and differentiation, which is the target of MAPK signal transduction inhibition. MEK1/2 signaling hyperactivation occurs frequently in malignant tumors, and thus can be used as a target for anti-cancer therapy (9,10). Targeting MEK has been shown to impair DNA damage repair pathways, and sensitize tumor cells to radiotherapy and chemotherapy. It has been shown that in pancreatic cancer, MEK inhibitors have been shown to interfere with the HR and non-homologous end-joining (NHEJ) pathways, thereby making pancreatic cancer cells more sensitive to radiotherapy and chemotherapy (11).

Apatinib can highly selectively inhibit vascular endothelial growth factor receptor 2 (*VEGFR-2*), and the inhibition of *VEGFR-2* leads to the inhibition of downstream phosphorylated extracellular signal-regulated kinases (12). Research has shown that the inhibition of VEGF-induced *VEGFR2/RAF/MEK/ERK1/2* signaling affects tumor cell growth in cholangiocarcinoma cells and pancreatic cancer cells (13,14).

RAD51 is an important protein for HR repair. The increased number and size of foci are associated with genomic damage (15). Research has shown that *MEK* inhibition reduces the formation of the HR marker *RAD51*, thereby enhancing DNA damage after olaparib treatment (16).

Thus, we sought to combine the antiangiogenic drug apatinib and PARP inhibitor fluzoparib to preliminarily analyze the mechanism of their combined therapeutic effect. We present this article in accordance with the ARRIVE reporting checklist (available at https://tcr.amegroups.com/article/view/10.21037/tcr-2025-666/rc).

Methods

Cell experiments

Cell culture and drugs

The human ovarian cancer cell line SKOV3 was purchased from Shanghai Mingjin Biological Co., LTD. (Shanghai, China). SKOV3 is an HRP-type ovarian cancer cell (17). The cells were maintained in McCoy's 5A (Gibco, Massachusetts, USA) medium supplemented with 1% double antibody (Seven Biotech Co., Ltd., Beijing, China) and 10% fetal bovine serum (Gibco). The cells were placed and cultured in an incubator at a constant temperature of 37 ℃ and 5% CO_2.

Both apatinib and fluzoparib were donated by Jiangsu Hendray Pharmaceutical Co., LTD. (Jiangsu, China). Cisplatin for injection (the freeze-dried type) was purchased from Qilu Pharmaceutical Co., LTD. (Shandong, China).

Cell viability was measured by MTT assay

The SKOV3 cells were spread into 96-well plates at 7×10^3 cells per well. According to the results of the preliminary experiment, the optimal concentration and time of administration were determined. The adherent cells were then treated with apatinib (8, 16, 32, and 64 μmol/L) and fluzoparib (148.15, 222.22, 333.33, and 500.00 μmol/L) for 48 hours. Cell viability was measured by MTT assay.

Drug grouping and cell specimen collection

The drug combination concentration was determined based on the cell viability assay results described above. The SKOV3 cells in the logarithmic growth phase were spread in 96- and 6-well plates for culturing. After adherence, the cells were divided into the control group, cisplatin group (10 μg/mL) (18), apatinib group (64 μmol/L), fluzoparib group (300 μmol/L), and apatinib (64 μmol/L) combined with fluzoparib (300 μmol/L) group. The drug acts for 48 hours. Apatinib is easy to precipitate and has a poor dose-response relationship. For the western blot experiments, apatinib was used at three different concentration gradients (16, 32, and 64 μmol/L) to enable a comprehensive molecular analysis to be conducted. Finally, the cell precipitates in the 6-well plates were collected and stored at −80 ℃ for the subsequent western blot experiments.

MTT and scratch assays were used to evaluate the effects of the drug combination

Experimental grouping was performed as described in "Drug grouping and cell specimen collection". The effect of the drug combination on cell proliferation was evaluated by MTT assay. The effect of the drug combination on cell migration was evaluated by scratch assay. In the cell-scratch experiment, the cells were cultured in an incubator for 24 h and then placed under an inverted digital biomicroscope to observe the cell migration in the same field of view at 0 h after scratching, and take pictures. Software was used to calculate the cell-scratch area to compare cell mobility between drug combination group and the rest of the group.

Western blot was used to detect the expression of *p-MEK*, *RAD51*, and *γH2AX* in each group

The cell precipitates collected in "Drug grouping and cell specimen collection" were lysed on ice and centrifuged to collect the supernatant. The protein concentration

was measured in accordance with the instructions of the bicinchoninic acid assay (BCA) protein quantification kit (Seven Biotech Co., Ltd, Beijing, China) for subsequent experiments. The proteins *P-MEK*, *RAD51*, and *γH2AX* were incubated to obtain corresponding band pictures (antibody from Abcam, Washington, USA).

Animal experiments

Establishment of subcutaneous tumor model and the *in vivo* study

In total, 30 female nude mice (Vital River Laboratory Animal Technology Co., Ltd, Beijing, China), aged 4 to 6 weeks, were used to establish cell-derived xenograft models. The SKOV3 cells in the logarithmic growth phase were measured. The cells were digested with trypsin and resuspended in phosphate buffered saline. A suspension of 2×10^7 cells per mL was prepared. The nude mice were subcutaneously injected with 2×10^6 cells (i.e., 100 uL of the cell suspension) in the mid-posterior axilla. Randomization was performed approximately 2 weeks after inoculation when the tumor diameter reached approximately 0.5 cm (n=6). The groups received normal saline, intraperitoneal cisplatin (3 mg/kg, Q3D), apatinib (100 mg/kg/bid) and fluzoparib (30 mg/kg/bid), or apatinib (100 mg/kg/bid) combined with fluzoparib (30 mg/kg/bid). The treatment period was 14 days.

Tumor growth status was observed daily during the drug intervention. Body weight, and long and short tumor diameters were measured regularly. Tumor volume (V) was calculated as follows: V = long diameter × short diameter 2 × 0.5 (unit: mm^3). The volume was plotted as a function of days. At the end of the treatment period, the nude mice in each group were sacrificed after drug anesthesia, and the tumor tissues were isolated and weighed. The tumor growth inhibition (TGI) rate was calculated as follows: TGI = (1 – T/C) ×100%, where T represents the mean tumor weight of the treatment group, and C represents the mean tumor weight of the control group. The liver and kidney were dissected and weighed to calculate the organ index, which was calculated as follows: organ index (%) = [(organ weight)/(mouse weight)] × 100%. The organs were embedded in paraffin sections, and stained with hematoxylin and eosin (HE). After dissection, half of the subcutaneous tumor tissue was stored at –80 ℃ for the subsequent western blot experiments, and the other half was fixed for 24 h and used for immunohistochemical detection. Animal experiments were performed under a project license (No. 2023035) granted by ethics board of Shanxi Province Cancer Hospital Animal Experiment, in compliance with institutional guidelines for the care and use of animals. A protocol was prepared before the study without registration.

Western blot was used to detect the expression of *p-MEK*, *RAD51*, and *γH2AX* in the subcutaneous tumors of each group

The subcutaneous tumor tissue was ground and lysed on ice to collect the supernatant by centrifugation. The concentration was measured in accordance with the instructions of the BCA protein quantification kit for the subsequent experiments. The proteins *p-MEK*, *RAD51*, and *γH2AX* were incubated to obtain corresponding band pictures.

Immunohistochemistry (IHC) was used to detect the expression of *γH2AX*, *p-ERK*, and *BRCA1* in the subcutaneous tumors

The subcutaneous tumor tissue fixed with fixative was made into paraffin sections. The expression of *p-ERK*, HR pathway-related protein *BRCA1*, and DNA damage marker *γH2AX* in the tumor tissues was detected by IHC. The immunostaining for *BRCA1*, *p-ERK*, and *γH2AX* was evaluated at ×400 magnification in at least three regions. Immunoreactivity was assessed semi-quantitatively based on staining intensity and proportion. There are divided into 4 grades according to the intensity of cell staining: high positive (sepia): 3 points; positive (brown): 2 points; low positive (faint yellow): 1 points; and negative (no positive coloration): 0 point. The different scores were then multiplied with the corresponding percentages of positive cells to determine the immunoreactivity score for each sample.

Statistical analysis

The western blot and IHC results were processed with Fiji-ImageJ software, version 1.53c (https://imagej.net/software/fiji/). GraphPadPrism (GraphPadPrism, version 9.5.0(525) for MacOSX, GraphPadSoftware, SanDiego, CA, USA) was used for the data analysis and mapping. The quantitative data are expressed as the mean ± standard deviation. The *t*-test was used for comparisons between two groups, and an analysis of variance was used for comparisons between multiple groups. A P value <0.05 was considered statistically significant.

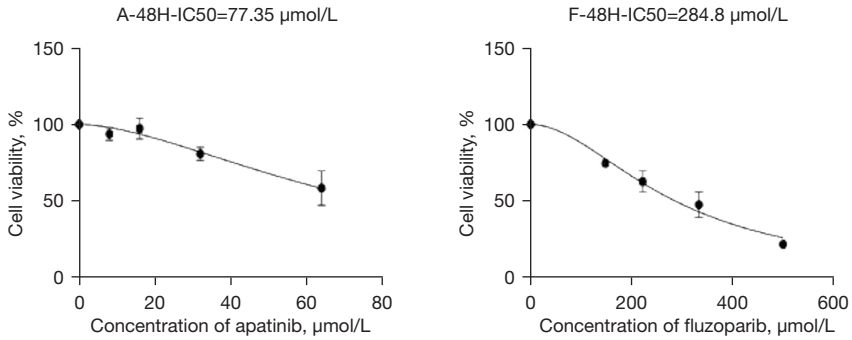

Figure 1 Effects of apatinib and fluzoparib at different drug concentrations on the proliferation rate of SKOV3 cells for 48 h (N=5). A, apatinib; F, fluzoparib; IC50, half maximal inhibitory concentration.

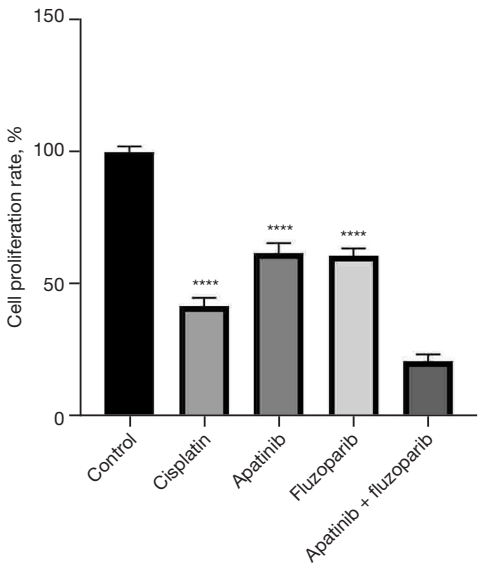

Figure 2 MTT assay results of the effects of different drugs on the cell proliferation rate at 48 h (N=5). When compared with the fluzoparib plus apatinib group: ****, indicates a statistically significant difference of P<0.0001. MTT, 3-(4,5-dimethyl-2-thiazolyl)-2,5-diphenyl-2-H-tetrazolium bromide.

Results

Effects of apatinib combined with fluzoparib on the ovarian cancer SKOV3 cells

Effects of different concentrations of apatinib and fluzoparib on the proliferation of the ovarian cancer SKOV3 cells

Both apatinib and fluzoparib inhibited cell proliferation in a dose-dependent manner (*Figure 1*). According to the MTT results, the half maximal inhibitory concentration (IC50) values of apatinib and fluzoparib at 48 h were 77.35 and 284.8 μmol/L, respectively. Therefore, 64 μmol/L of apatinib and 300 μmol/L of fluzoparib were selected for the subsequent experiments according to the IC50 values of cells.

Effects of apatinib combined with fluzoparib on the proliferation and migration ability of ovarian cancer SKOV3 cells

The effects of the different drugs on the proliferation of SKOV3 cells are shown in *Figure 2*. Compared with a single drug, apatinib combined with fluzoparib significantly inhibited cell proliferation (P<0.05). These results indicate that combination therapy is more effective than monotherapy.

The effect of apatinib combined with fluzoparib on the migration ability of SKOV3 cells was verified by cell-scratch assay. The results are shown in *Figure 3*. Cisplatin, apatinib, and fluzoparib significantly inhibited the migration ability of the SKOV3 cells. Among the treatments, the combined treatment had the most significant inhibitory effect on the migration ability of the tumor cells. Additionally, the effect of apatinib combined with fluzoparib was better than that of cisplatin, apatinib, and fluzoparib alone, and the difference was statistically significant (P<0.05).

Effects of apatinib combined with fluzoparib on *p-MEK*, *RAD51*, and *γ-H2AX* in the SKOV3 cells

The western blot results are shown in *Figure 4*. Compared with the apatinib combined with fluzoparib group, *γH2AX* protein expression was significantly decreased in the apatinib monotherapy group (P<0.05). Compared with the control group, *RAD51* and *p-MEK* expression was significantly decreased in the apatinib combined with

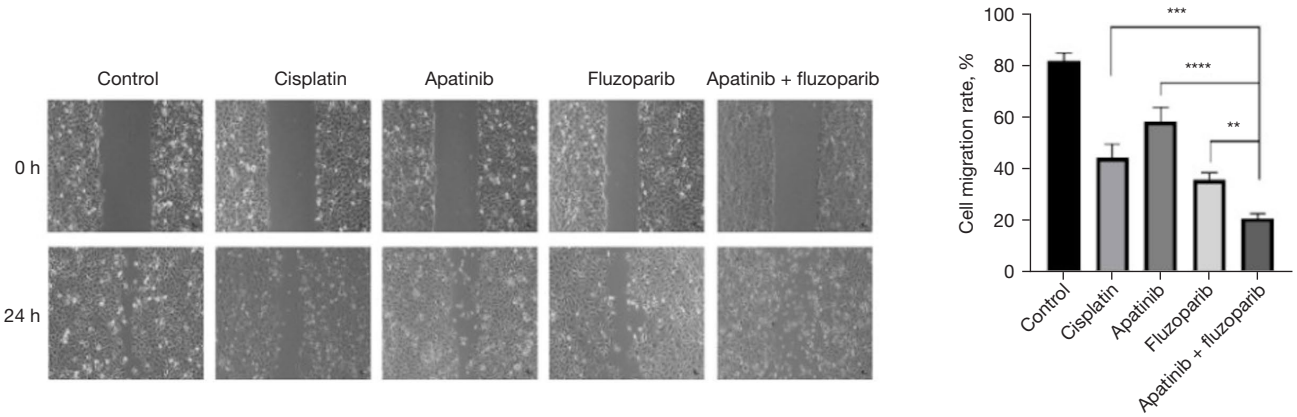

Figure 3 Wound-healing results of the SKOV3 cells treated with different drugs (N=3). Observe the same position at ×100 magnification. Compared with the combination drug group (i.e., the apatinib plus fluzoparib group): **, indicates a statistically significant difference of P<0.01; ***, indicates a statistically significant difference of P<0.001; ****, indicates a statistically significant difference of P<0.0001.

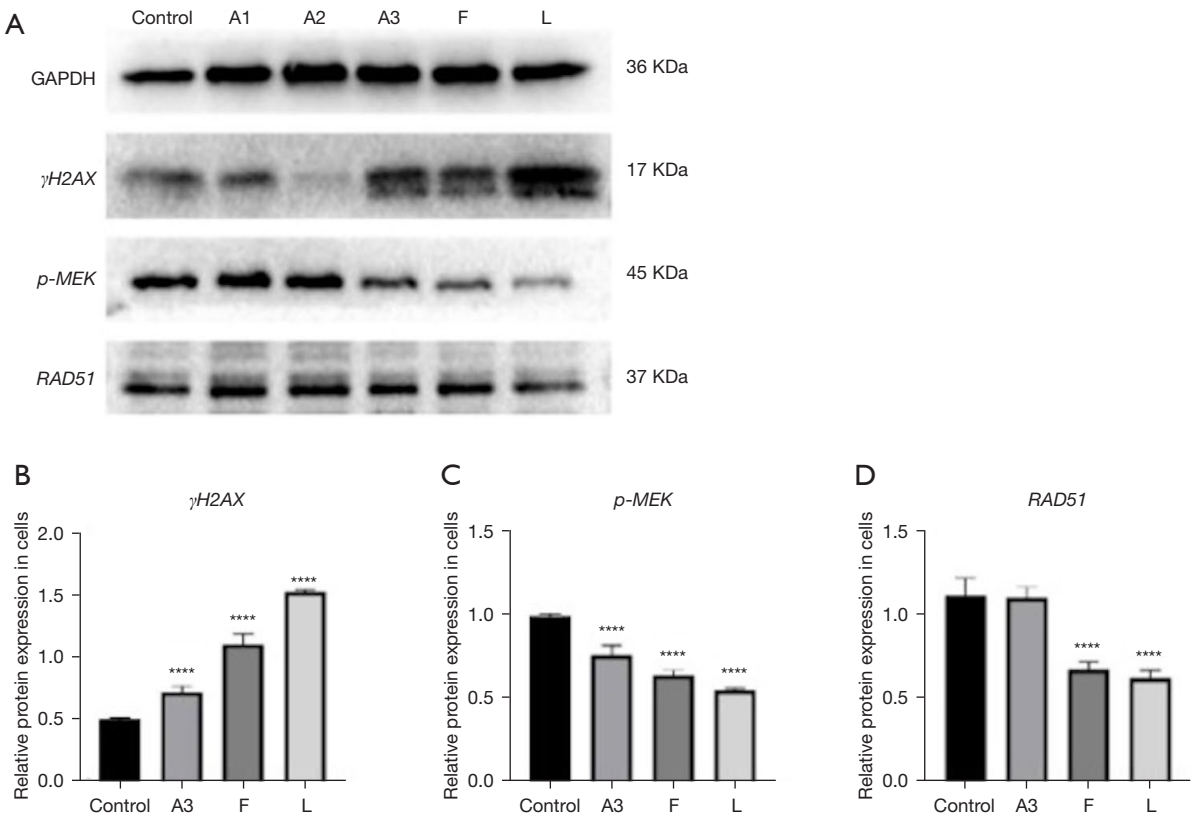

Figure 4 Effects of different drugs on the protein expression levels of *γH2AX*, *p-MEK*, and *RAD51* in the SKOV3 cells (N=3). (A) Raw protein expression for each indicator. (B) Expression statistics of the protein *γH2AX*. (C) Expression statistics of the protein *p-MEK*. (D) Expression statistics of the protein *RAD51*. A1: 16 μmol/L; A2: 32 μmol/L; A3: 64 μmol/L of apatinib; F: 300 μmol/L of fluzoparib; L: 64 μmol/L of apatinib combined with 300 μmol/L of fluzoparib. Compared with the control group, ****, indicates a statistically significant difference of P<0.0001.

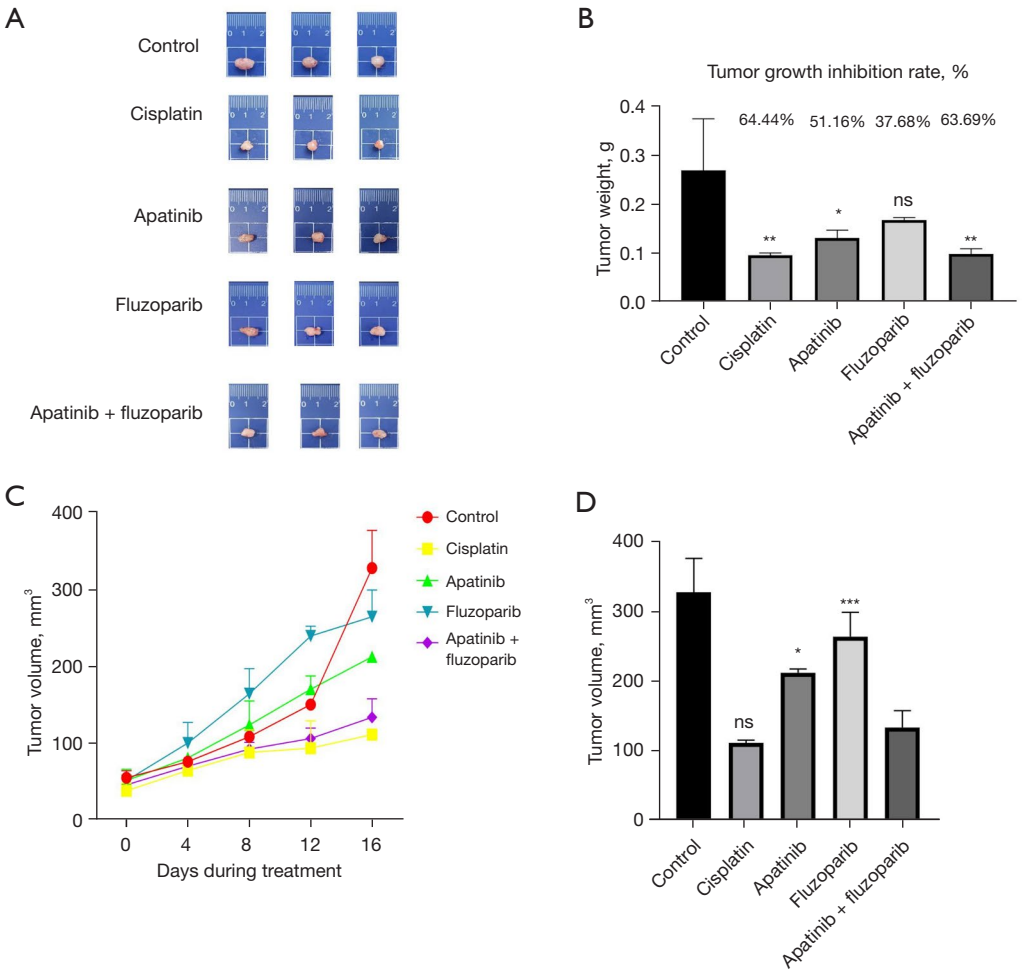

Figure 5 Effects of the different drugs in the subcutaneous tumor models in nude mice (typical picture) (N=6). Data are presented as the mean ± standard deviation. (A) Photographs of exfoliated tumors obtained at the end of treatment. (B) Plot of tumor weight by drug group. Compared with the control group: ns indicates no statistically significant difference; *, indicates a statistically significant difference of P<0.05; **, indicates a statistically significant difference of P<0.01. (C) Plot of tumor volume versus days of treatment. (D) The last tumor volume map of different drug groups. Compared with the apatinib combined with fluzoparib group: ns indicates no statistically significant difference, * indicates a statistically significant difference of P<0.05; ***, indicates a statistically significant difference of P<0.001.

fluzoparib group (P<0.05). Thus, we hypothesized that the combination of apatinib and fluzoparib may down-regulate the expression of HR pathway-related protein *RAD51* by reducing the expression of *MEK* phosphorylation signaling and up-regulate the expression of DNA damage-related protein *γH2AX*.

Effects of apatinib combined with fluzoparib in the SKOV3 cell-line xenograft tumor model

Apatinib combined with fluzoparib inhibits the growth of the SKOV3 cell-line transplanted tumor model

The results of the *in vivo* experiments are shown in *Figure 5*. At the end of the treatment, the nude mice were sacrificed. *Figure 5A* shows an anatomical diagram. *Figure 5B* shows the tumor weight after dissection. Compared with that of the control group, the tumor weights of the cisplatin group, apatinib group, and apatinib combined with fluzoparib group were significantly reduced (P<0.05). As *Figure 5C* shows, the tumor volume of the control and drug-treated mice increased progressively as the treatment days increased. As *Figure 5D* shows, in the final tumor volume determined after the end of the final experiment, the tumor volume of the mice receiving the combined treatment was significantly smaller than that of

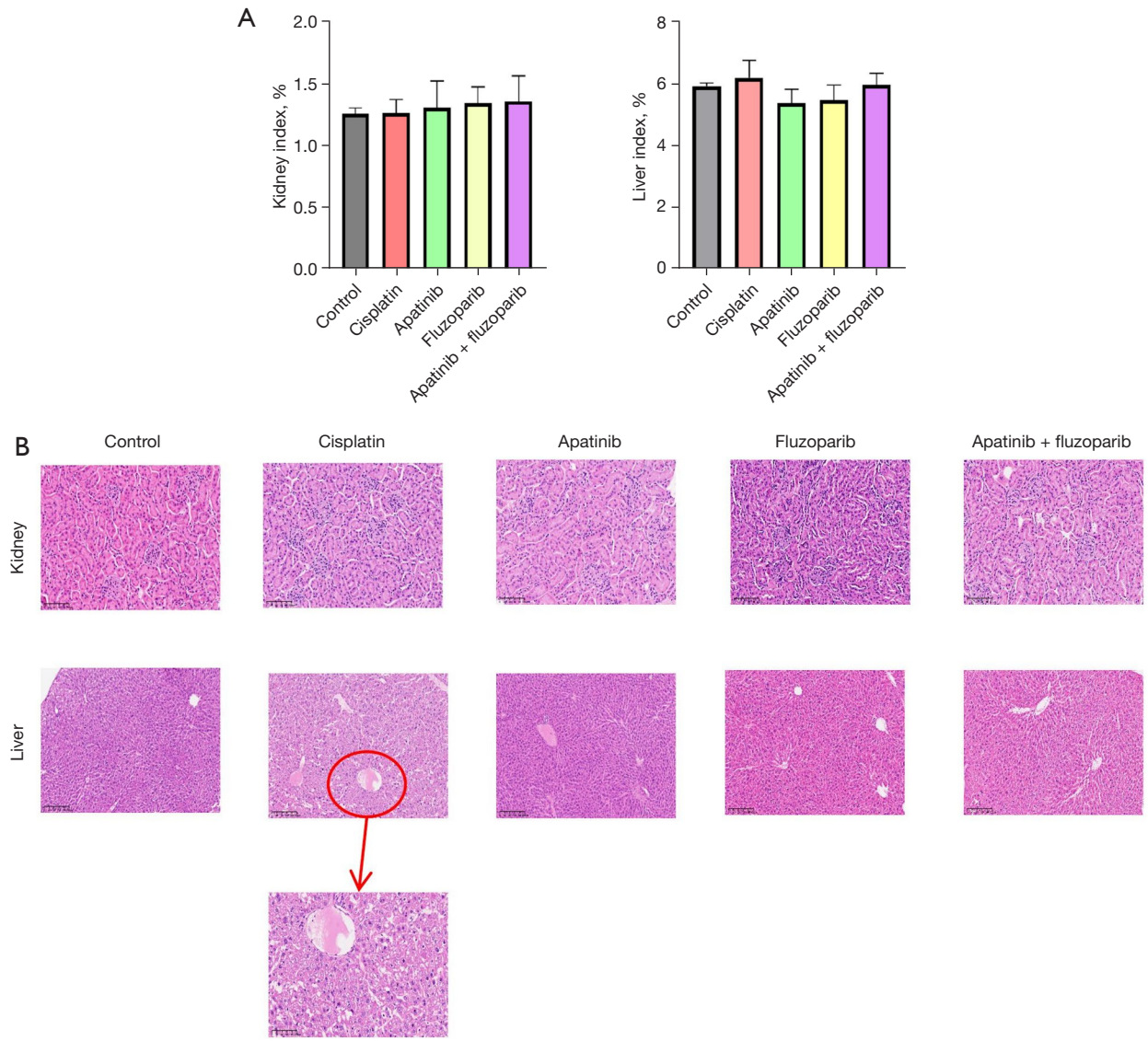

Figure 6 *In vivo* toxicity analysis of drugs (N=3). The kidneys of each group were observed at ×200 magnification; the livers were observed at ×100 magnification, and the liver damage in the cisplatin group was observed with ×200 magnification. (A) Kidney/liver organ index in the nude mice. The data are presented as the mean ± standard deviation. (B) HE staining of liver and kidney of nude mice. The HE staining of nude mice organs showed liver damage in the cisplatin group. HE, hematoxylin and eosin.

the other three treatment groups (P<0.05), and there was no significant difference between the combined treatment group and the cisplatin group. These results indicate that apatinib combined with fluzoparib effectively inhibited the growth of the SKOV3 cell-line xenograft tumor model.

In vivo toxicity analysis of apatinib combined with fluzoparib

The results of the *in vivo* toxicity analysis are shown in *Figure 6A,6B*. *Figure 6A* shows the organ index of the liver and kidney, which is an indicator to evaluate the relative weight of organs, which can quickly assess the effect of

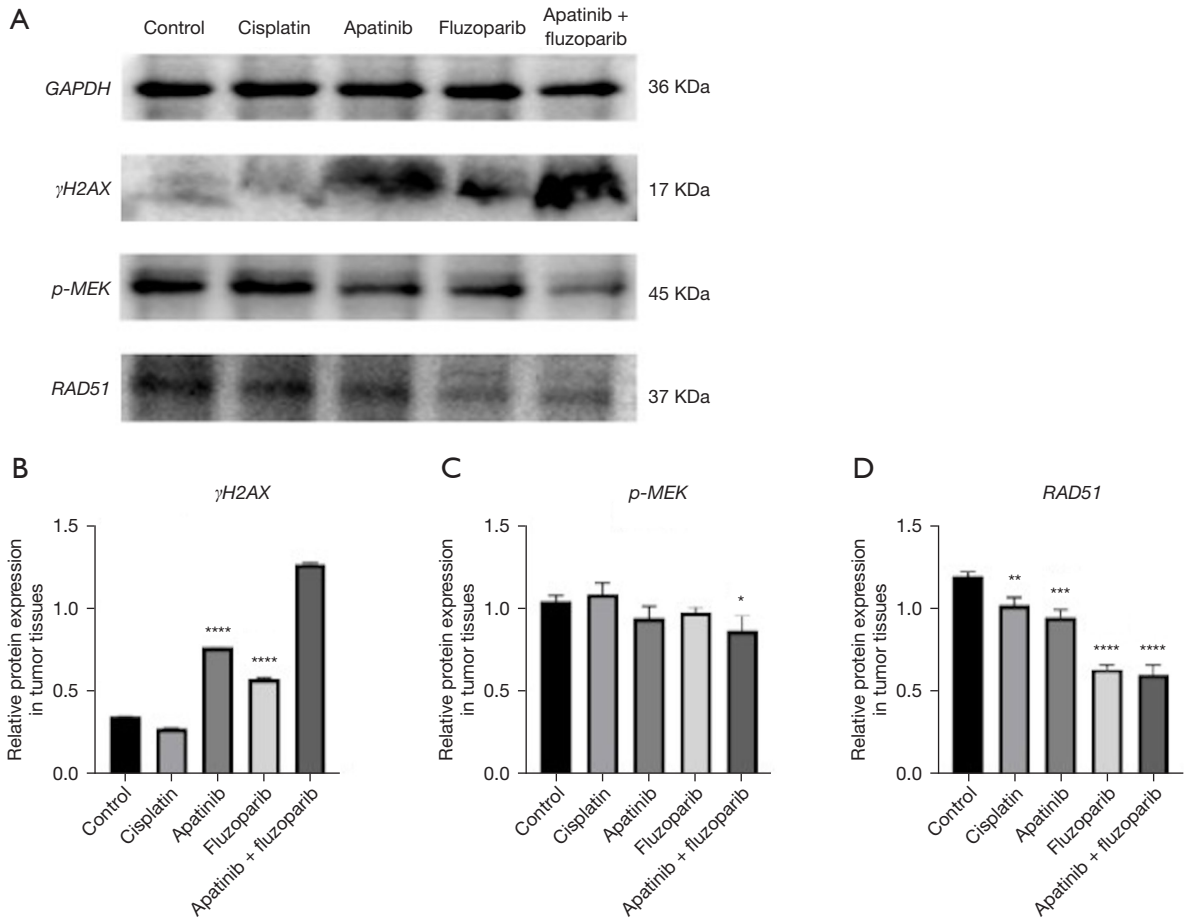

Figure 7 Effects of different drugs on *γH2AX* (A), *p-MEK* (B) and *RAD51* (C) protein expression *in vivo* (N=3). (A) Raw protein expression for each indicator. (B) Expression statistics of the protein *γH2AX*. (C) Expression statistics of the protein *p-MEK*. (D) Expression statistics of the protein *RAD51*. Compared with the control group: *, indicates a statistically significant difference of P<0.05; **, indicates a statistically significant difference of P<0.01; ***, indicates a statistically significant difference of P<0.001; ****, indicates a statistically significant difference of P<0.0001.

drugs on specific organs. There was no significant difference in organ index between groups. HE staining in *Figure 6B* showed that there was no obvious organ toxicity in the drug treatment, and only partial liver damage was observed in the cisplatin group.

Western blot was used to detect the effects of apatinib combined with fluzoparib on *p-MEK*, *RAD51*, and *γ-H2AX* in the xenograft model of the SKOV3 cell line

Western blot was used to detect the changes of the corresponding indexes in the transplanted tumor model. The western blot results are shown in *Figure* 7. Compared with the single-drug groups, the expression of the DNA damage marker *γH2AX* protein in the apatinib combined with fluzoparib group was significantly increased (P<0.05), indicating that the combination of apatinib and fluzoparib had the greatest effect on DNA damage in the mice. Compared with the control group, the apatinib combined with fluzoparib group showed a significant reduction in the expression of *p-MEK* (P<0.05).

IHC was used to detect the effects of apatinib combined with fluzoparib on *γ-H2AX*, *p-ERK*, and *BRCA1* in the xenograft model of SKOV3 cell line

Changes in the corresponding indexes of the transplanted tumor model were detected by IHC. The IHC experiment results are shown in *Figure 8*. Compared with the control group, the apatinib combined with fluzoparib group showed

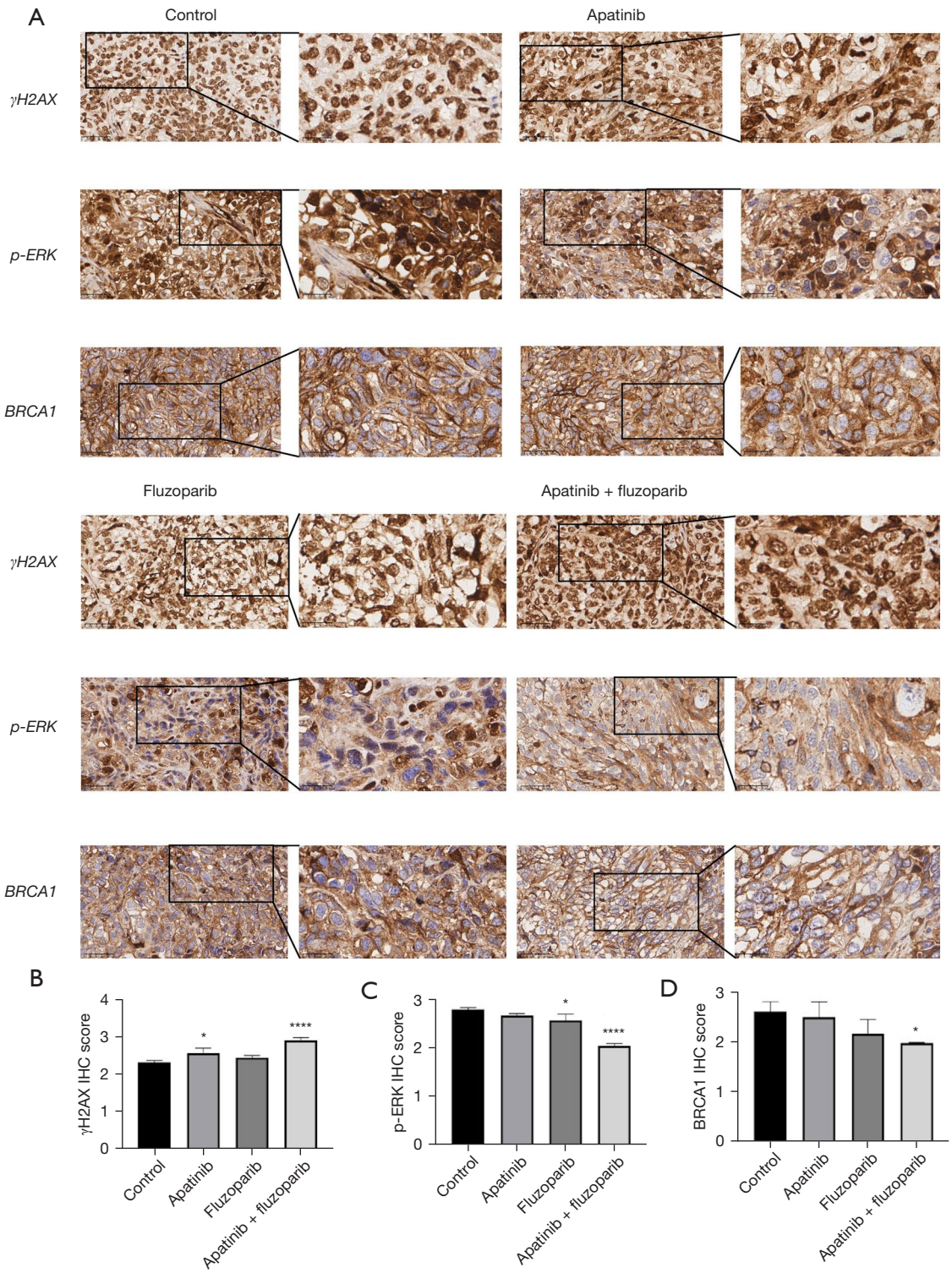

Figure 8 Effects of different drugs on *γH2AX*, *p-ERK*, *BRCA1*, and protein expression *in vivo*. The overall figure was observed at ×400 magnification and the local at ×800 magnification (Nuclear staining) (N=3). (A) Raw protein expression for each indicator. (B) Expression statistics of the protein *γH2AX*. Compared with the control group, * indicates statistically significant difference, P<0.05, **** indicates statistically significant difference, P<0.0001. (C) Expression statistics of the protein *p-ERK*. (D) Expression statistics of the protein *BRCA1*. Compared with the control group: *, indicates statistically significant difference of P<0.05; ****, indicates statistically significant difference of P<0.0001.

a significant increase in the expression of the DNA damage marker γ*H2AX* protein (P<0.05), and a significant reduction in the expression of *p-ERK* and *BRCA1* (P<0.05).

Discussion

At present, "chemotherapy-free" therapies are mostly focused on PARP inhibitors. PARP inhibitors are not only used in the maintenance treatment of ovarian cancer, but are also expected to "replace chemotherapy" as a new "chemotherapy-free" treatment mode for patients. Moreover, compared with traditional chemotherapy, targeted therapy has the advantages of strong specificity and clear targets. The FZOCUS-3 trial, which involved patients with g*BRCA*-mutated platinum-sensitive recurrent ovarian cancer who had received 2–4 lines of platinum-based chemotherapy, reported a promising treatment effect with fluzoparib (19). Nearly 75% of the non-g*BRCA* patients have a urgent need for diagnosis and treatment. Therefore, the combination of fluzoparib and anti-vascular drugs will be an effective treatment.

Our cell experiments showed that apatinib combined with fluzoparib had a better inhibitory effect on cell growth than either drug alone. It also significantly inhibited SKOV3 cell migration. The western blot results showed that the combination of apatinib and fluzoparib significantly inhibited the phosphorylation of the *MEK* protein, and then down-regulated the expression of the HR pathway-related protein *RAD51*. Finally, the expression of DNA damage-related protein γ*H2AX* in the ovarian cancer cells was aggravated.

Similarly, our experimental results showed that apatinib combined with fluzoparib significantly inhibited subcutaneous tumor growth in the SKOV3 mice. No significant *in vivo* toxicity was observed, and the corresponding liver injury was only observed in the cisplatin group. The western blot results showed that the combined treatment significantly increased the expression of DNA damage-related protein γ*H2AX*, and had a weak inhibitory effect on the expression of *p-MEK* in the *MAPK* pathway.

The IHC results also confirmed that apatinib combined with fluzoparib significantly increased the expression of DNA damage-related protein γ*H2AX*. The phosphorylation of *ERK*, a downstream protein of *MEK*, and *BRCA1*, a HR pathway-related protein, were down-regulated.

Taken together, we concluded that the effect of apatinib combined with fluzoparib on the HR pathway was mediated by the inhibition of *MEK* signaling in the *MAPK* pathway, which resulted in the down-regulation of the HR pathway-related proteins *RAD51* and *BRCA1*. Finally, combinations medications enhanced the expression of the DNA damage-related protein γ*H2AX* and exerted a killing effect on the tumor cells. However, our research results and research depth are preliminary, and the expression of downstream signals in the *MAPK* pathway and the deep mechanism need to be further verified by corresponding experiments.

Conclusions

In this study, we demonstrated by *in vivo* and *in vitro* experiments that apatinib combined with fluzoparib significantly inhibited the growth of SKOV3 lineage ovarian cancer, producing a better tumor suppression effect than apatinib and fluzoparib alone. The mechanism of action may be through the inhibition of *MEK* signaling in the *MAPK* pathway, which led to the down-regulation of the HR pathway-related proteins *RAD51* and *BRCA1*, and significantly increased the expression of the DNA damage-related protein γ*H2AX*. We provide a rationale for clinical drug combinations that expand the scope of PARP inhibitors and provide an emerging "chemotherapy-free" option for HRP ovarian cancer patients.

Acknowledgments

None.

Footnote

Reporting Checklist: The authors have completed the ARRIVE reporting checklist. Available at https://tcr.amegroups.com/article/view/10.21037/tcr-2025-666/rc

Data Sharing Statement: Available at https://tcr.amegroups.com/article/view/10.21037/tcr-2025-666/dss

Peer Review File: Available at https://tcr.amegroups.com/article/view/10.21037/tcr-2025-666/prf

Funding: This work was supported by Shanxi Provincial Key Research and Development Program (No. 201903D321174 to H.Z.) and the Scientific and Educational Cultivation Fund of the National Oncology Regional Medical Center (SD2023029 to H.Z.).

Conflicts of Interest: All authors have completed the ICMJE uniform disclosure form (available at https://tcr.amegroups.com/article/view/10.21037/tcr-2025-666/coif). The authors have no conflicts of interest to declare.

Ethical Statement: The authors are accountable for all aspects of the work in ensuring that questions related to the accuracy or integrity of any part of the work are appropriately investigated and resolved. Animal experiments were performed under a project license (No. 2023035) granted by ethics board of Shanxi Province Cancer Hospital Animal Experiment, in compliance with institutional guidelines for the care and use of animals.

References

1. Siegel RL, Giaquinto AN, Jemal A. Cancer statistics, 2024. CA Cancer J Clin 2024;74:12-49.
2. Luo Y, Xia Y, Liu D, et al. Neoadjuvant PARPi or chemotherapy in ovarian cancer informs targeting effector Treg cells for homologous-recombination-deficient tumors. Cell 2024;187:4905-4925.e24.
3. Morand S, Devanaboyina M, Staats H, et al. Ovarian Cancer Immunotherapy and Personalized Medicine. Int J Mol Sci 2021;22:6532.
4. Gynecologic Oncology Group of Minimally Invasive and Noninvasive Medicine Committee of Chinese Medical Doctor Association;Holistic Integrative Ovarian Cancer Committee of China Anti-Cancer Association. Chinese expert consensus on diagnosis and treatment of platinum-sensitive recurrent ovarian cancer(2023 edition). Chinese Journal of Practical Gynecology and Obstetrics 2023;39:935-42.
5. Vanacker H, Harter P, Labidi-Galy SI, et al. PARP-inhibitors in epithelial ovarian cancer: Actual positioning and future expectations. Cancer Treat Rev 2021;99:102255.
6. Liu JF, Barry WT, Birrer M, et al. Combination cediranib and olaparib versus olaparib alone for women with recurrent platinum-sensitive ovarian cancer: a randomised phase 2 study. Lancet Oncol 2014;15:1207-14.
7. Pu T, Zhang C, Su B, et al. Research progress in intratumoral heterogeneity and clinical significance of ovarian cancer. Medicine (Baltimore) 2024;103:e36074.
8. Guo Q, Wu X. Progress in diagnosis and treatment of ovarian cancer in 2022. Journal of Multidisciplinary Cancer Management (Electronic Version) 2023,9:110-8.
9. Burotto M, Chiou VL, Lee JM, et al. The MAPK pathway across different malignancies: a new perspective. Cancer 2014;120:3446-56.
10. Caunt CJ, Sale MJ, Smith PD, et al. MEK1 and MEK2 inhibitors and cancer therapy: the long and winding road. Nat Rev Cancer 2015;15:577-92.
11. Estrada-Bernal A, Chatterjee M, Haque SJ, et al. MEK inhibitor GSK1120212-mediated radiosensitization of pancreatic cancer cells involves inhibition of DNA double-strand break repair pathways. Cell Cycle 2015;14:3713-24.
12. Li J, Qin S, Xu J, et al. Apatinib for chemotherapy-refractory advanced metastatic gastric cancer: results from a randomized, placebo-controlled, parallel-arm, phase II trial. J Clin Oncol 2013;31:3219-25.
13. Hu Y, Jing J, Shi Y, et al. Apatinib inhibits pancreatic cancer growth, migration and invasion through the PI3K/AKT and ERK1/2/MAPK pathways. Transl Cancer Res 2021;10:3306-16.
14. Huang M, Huang B, Li G, et al. Apatinib affect VEGF-mediated cell proliferation, migration, invasion via blocking VEGFR2/RAF/MEK/ERK and PI3K/AKT pathways in cholangiocarcinoma cell. BMC Gastroenterol 2018;18:169.
15. Laurini E, Marson D, Fermeglia A, et al. Role of Rad51 and DNA repair in cancer: A molecular perspective. Pharmacol Ther 2020;208:107492.
16. Vena F, Jia R, Esfandiari A, et al. MEK inhibition leads to BRCA2 downregulation and sensitization to DNA damaging agents in pancreas and ovarian cancer models. Oncotarget 2018;9:11592-603.
17. Wilson AJ, Sarfo-Kantanka K, Barrack T, et al. Panobinostat sensitizes cyclin E high, homologous recombination-proficient ovarian cancer to olaparib. Gynecol Oncol 2016;143:143-51.
18. Yang Y, Gao L, Zhao H. Effect of apatinib combined with fluzoparib on proliferation ability of human ovarian

cancer cisplatin-resistant cells. Cancer Research and Clinic 2023;7:494-9.
19. Li N, Bu H, Liu J, et al. An Open-label, Multicenter, Single-arm, Phase II Study of Fluzoparib in Patients with Germline BRCA1/2 Mutation and Platinum-sensitive Recurrent Ovarian Cancer. Clin Cancer Res 2021;27:2452-8.

Cite this article as: Gao L, Wang S, Hu X, Wang L, Xi Y, Bu P, Zhao G, Zhao L, Yang Y, Zhao H. Preliminary study of apatinib combined with fluzoparib in the treatment of HRP ovarian cancer via the HR pathway. Transl Cancer Res 2025;14(4): 2470-2482. doi: 10.21037/tcr-2025-666